Monoallelic *ABCA4* Mutations Appear Insufficient to Cause Retinopathy: A Quantitative Autofluorescence Study

- Supplementary material -

Philipp L. Müller[1‡], Martin Gliem[1‡], Elisabeth Mangold[2], Hanno J. Bolz[3,4], Robert P. Finger[1,5], Myra McGuinness[5], Christian Betz[3], Zhichun Jiang[6], Bernhard H.F. Weber[7], Robert E. MacLaren[8], Frank G. Holz[1], Roxana A. Radu[6], Peter Charbel Issa[1*]

[1] *Department of Ophthalmology, University of Bonn, Bonn, Germany*
[2] *Institute of Human Genetics, University of Bonn, Bonn, Germany*
[3] *Bioscientia Center for Human Genetics, Ingelheim, Germany*
[4] *Institute of Human Genetics, University Hospital of Cologne, Cologne, Germany*
[5] *Centre for Eye Research Australia, University of Melbourne, Royal Victorian Eye and Ear Hospital, Melbourne, Australia*
[6] *Stein Eye Institute, Department of Ophthalmology, University of California at Los Angeles School of Medicine, Los Angeles, California, U.S.A.*
[7] *Institute of Human Genetics, University of Regensburg, Regensburg, Germany*
[8] *The Nuffield Laboratory of Ophthalmology & Oxford Biomedical Research Centre, University of Oxford, Oxford, UK*

‡ *Both authors contributed equally to this work*

Supplementary Figure 1: Emission spectrum of the fluorescence reference material at 488 nm excitation.

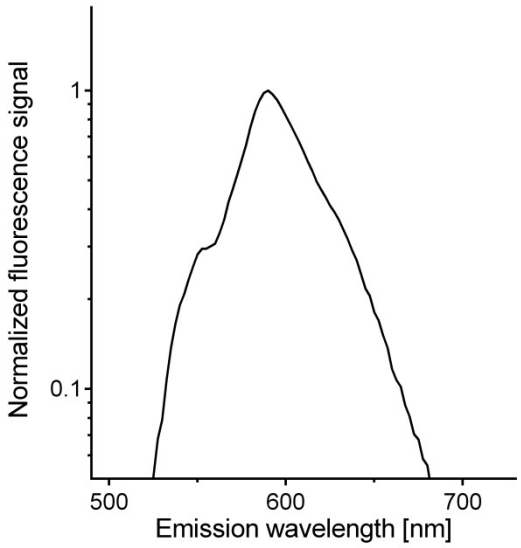

The normalized emission spectrum of the internal fluorescence reference material is shown (data kindly provided by Heidelberg Engineering). A laser beam at 488 nm was focused onto the internal reference and the emitted fluorescence light was separated by a special beam splitter from the exciting beam (constant reflectivity of about 85% for the spectral range 480 nm – 720 nm). A barrier filter with high transmission between 500 nm and 720 nm was used to remove the reflected 488 nm light. The fluorescence light was coupled into a 400 µm core diameter multimode fiber (constant transmission between 500 and 720 nm) and coupled into a spectrometer (USB4000-VIS-NIR, OceanOptics, Dunedin, USA). The background of the raw data was subtracted and the data was normalized to the peak emission at about 590 nm. The emission spectra of the internal references used in this study and by Delori et al. are comparable,[1] but narrower than the emission spectrum of lipofuscin.[1, 2]

Supplementary Figure 2: Comparison of controls with published data.

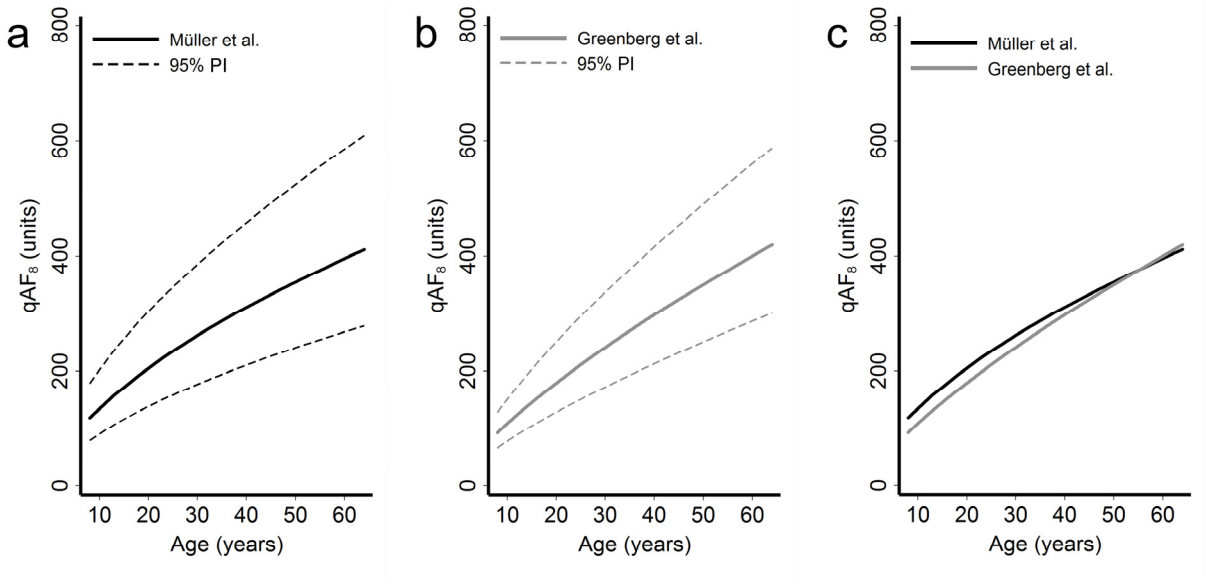

The graphs show the non-linear regression curve and the 95% prediction interval of the age-dependent qAF_8 values (dashed lines). To compare our data with published data by Greenberg et al.[3] the qAF_8 values of controls were fit using the following model: ln(qAF8)=3.329+0.657×ln(age)+e, which is equivalent to: qAF8=B×age^(0.657)+e, where B=27.921 (95% confidence interval 19.165, 40.676641) and e is the residual error (a). For Caucasian subjects, Greenberg et al fit their control data using the following model: qAF8=B×age^(0.732)+e, where B=19.98 (95% confidence interval 14.29, 27.95) and e is the residual error (b). In (c) the non-linear regression lines of (a) and (b) are overlaid. Using a Wald test of the linear hypothesis that the coefficients of our study were equal to those from Greenberg et al., there was a statistical evidence for a difference in the age coefficient (F(1,108)=8.69, P=0.004) and in the intercept coefficient (χ^2 (1)=10.68, P=0.001). However, visual comparison suggests a comparable distribution of controls.

Supplementary Figure 3: Conventional and quantitative fundus autofluorescence of each included family.

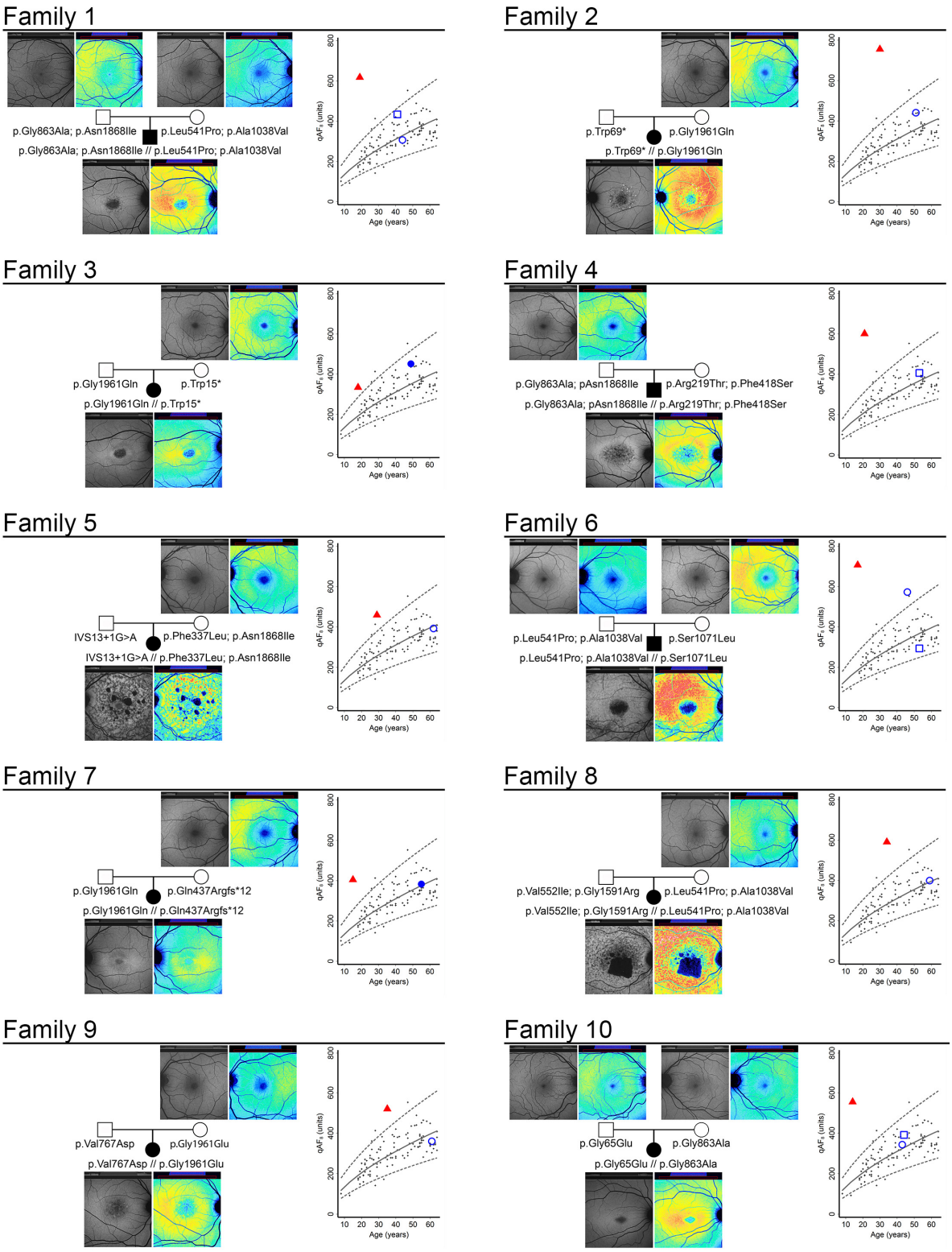

Supplementary Figure 3 (continued)

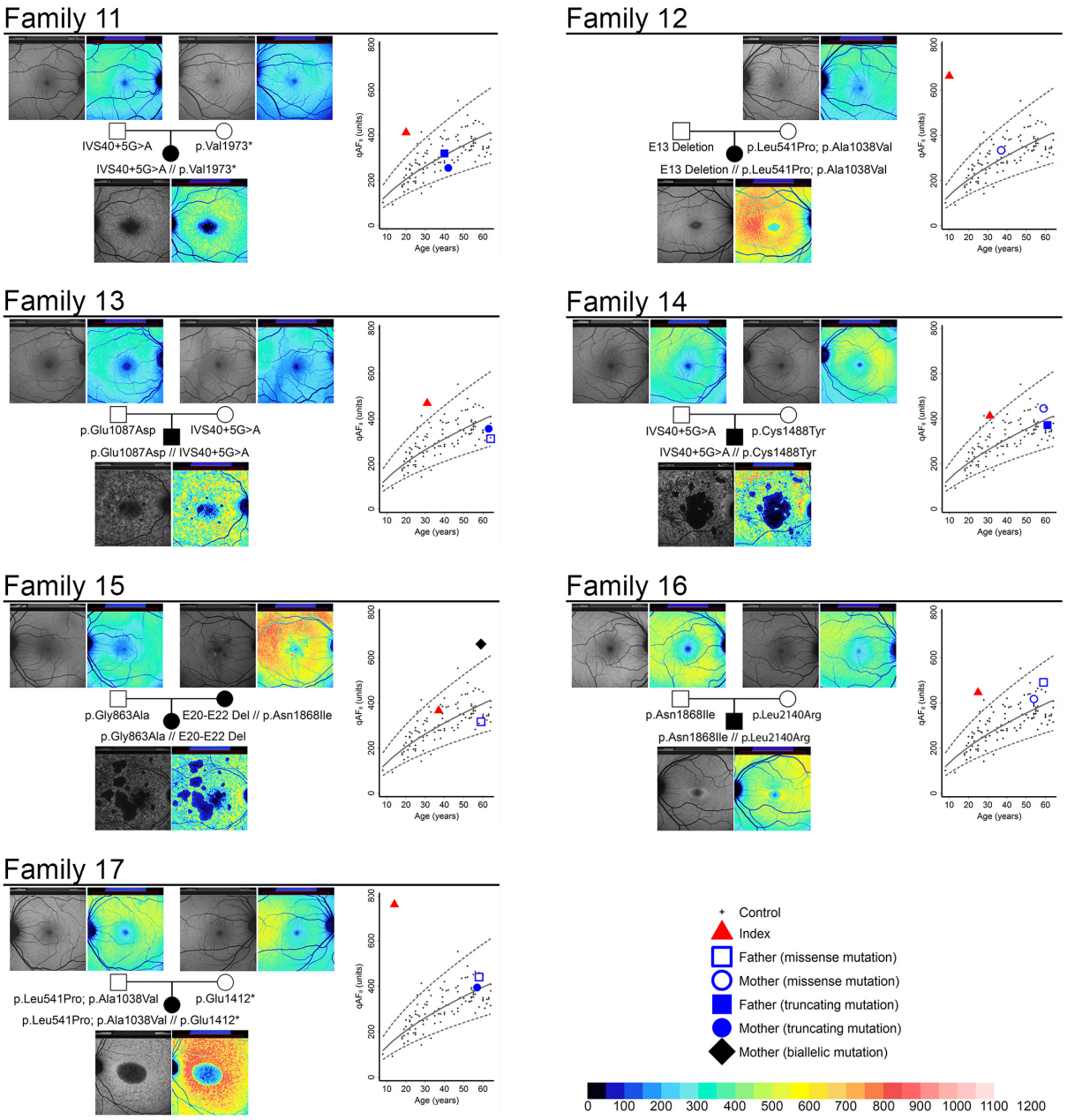

Fundus AF images (left) and corresponding color-coded quantitative AF (qAF) images (right) of all included index patients (bottom) and their parents (top). The graph to the right in each panel illustrates the qAF_8 of the index patients (red triangles) and their parents (blue squares and dots) with monoallelic *ABCA4*-mutations relative to the age-dependent 95% prediction interval (dashed lines) of normal controls (black crosses). qAF_8 values are usually high in index patients and within the normal range in their parents, who carry only one disease-causing *ABCA4* mutation.

Supplementary Figure 4: *N*-retinylidene-phosphatidylethanolamine (*N*-Ret-PE) levels in mouse eyes.

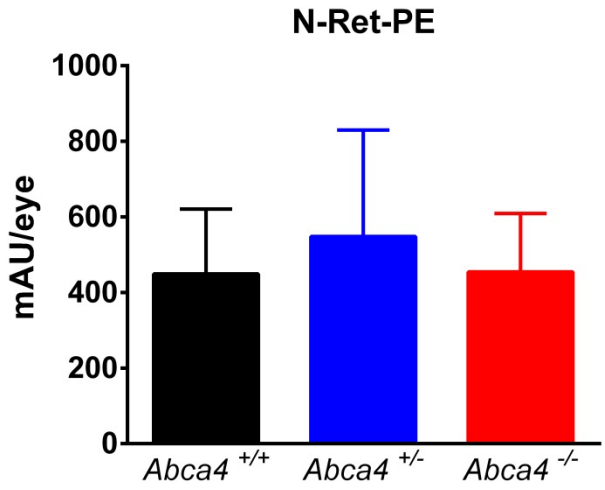

Levels of *N*-retinylidene-phosphatidylethanolamine (*N*-Ret-PE) were similar in all three groups (n=5-6). mAU/eye: milli absorbance units per eye.

Supplementary Table 1

Exon	Coding DNA	Protein	Effect	Prediction of Pathogenicity	HGMD Class	rs Number	Combined Allele Frequencies	dbSNP Clin. Asso.	PubMed ID
1	c.45G>A	p.Trp15*	stopgain	P(6/8) = F(2/4) + C(4/4)	Disease-causing mutation	rs62645957	0.00%	Yes	10090887
3	c.194G>C	p.Gly65Ala	missense	P(14/14) = F(8/8) + C(6/6)	Disease-causing mutation	NA	0.00%	NA	10206579
3	c.206G>A	p.Trp69*	stopgain	P(7/8) = F(3/4) + C(4/4)	NA	NA	0.00%	NA	NA
6	c.656G>C	p.Arg219Thr	missense	P(7/14) = F(3/8) + C(4/6)	Disease-causing mutation	rs61748537	0.00%	Yes	14517951
8	c.1009T>C	p.Phe337Leu	missense	P(8/14) = F(3/8) + C(5/6)	NA	NA	0.00%	NA	NA
10	c.1253T>C	p.Phe418Ser	missense	P(14/14) = F(8/8) + C(6/6)	Disease-causing mutation	NA	0.00%	NA	21911583
12	c.1622T>C	p.Leu541Pro	missense	P(14/14) = F(8/8) + C(6/6)	Disease-causing mutation	rs61751392	0.00% - 0.05%	Yes	9781034
12	c.1654G>A	p.Val552Ile	missense	P(7/14) = F(3/8) + C(4/6)	Disease-causing mutation	rs145525174	0.00% - 0.60%	NA	18024811
15	c.2300T>A	p.Val767Asp	missense	P(13/14) = F(7/8) + C(6/6)	Disease-causing mutation	rs61751395	0.00%	Yes	10711710
17	c.2588G>C	p.Gly863Ala	missense (SS)	P(11/14) = F(5/8) + C(6/6)	Disease-causing mutation	rs76157638	0.00% - 1.60%	Yes	9054934
21	c.3113C>T	p.Ala1038Val	missense	P(9/14) = F(3/8) + C(6/6)	Disease-causing mutation	rs61751374	0.00% - 0.20%	Yes	9054934
22	c.3212C>T	p.Ser1071Leu	missense	P(13/14) = F(7/8) + C(6/6)	Disease-causing mutation	rs61750065	0.00% - 0.02%	Yes	9973280
33	c.4771G>A	p.Gly1591Arg	missense (SS)	P(7/14) = F(2/8) + C(5/6)	Likely disease-causing mutation	rs113106943	0.00% - 0.82%	NA	24265693
40	c.5603A>T	p.Asn1868Ile	missense	P(9/14) = F(4/8) + C(5/6)	Disease-associated polymorphism, supporting functional evidence	rs1801466	2.08% - 7.10%	Yes	11328725
41	c.5714+5G>A	NA	splice donor	P(0/0) = F(0/0) + C(0/0)	Disease-causing mutation	rs61751407	0.00% - 0.10%	Yes	9466990
42	c.5882G>A	p.Gly1961Glu	missense	P(12/14) = F(7/8) + C(5/6)	Disease-causing mutation	rs1800553	0.00% - 2.50%	Yes	9295268

ABCA4 mutations and prediction of pathogenicity. Resulting total prediction **P** as sum of combined functional predictions **F** (by bioinformatic tools SIFT, PolyPhen-2, MutationTaster, MutationAssessor, fathmm, LRT, VEST, CADD) and combined conservation prediction **C** (by bioinformatic tools PhyloP, GERP++, phastCons, SiPhy). Combined allele frequencies were derived from databases dbSNP, 1000 Genomes Project (TGP), Exome Sequencing Project (ESP), Complete Genomics (CG69), National Cancer Institute (NCI-60), Genome of the Netherlands (GoNL), Exome Aggregation Consortium (ExAC). NA: not applicable; SS: potentially affecting splicing.

Supplementary Table 2

This Study		Previous Studies		
Variant (Amino Acid Change)	Age at examination	Variant (Amino Acid Change)	Age of Onset	Phenotype
Truncating mutations (stop, frame shift, deletions, or splice site mutations)				
c.5714+5G>A (splice)	63, 40	c.768G>T (splice)	45, 49, 56, 61, 65, 72	A
c.1309delC (p.Gln437Argfs*12)	55	c.4859_4864delATAACAinsTCCT (p.Asn1620fs)	50	B
c.5917delG (p.Val1973*)	42	c.4234C>T (p.Q1412*)	50	B
c.45G>A (p.Trp15*)	49	c.3874C>T (Gln1292*)	45	A
c.4234C>T (p.Glu1412*)	57	c.C450T (p.Arg152*)	70	E
E 20-22 deletion	59	5196+1G>T (splice)	83	A
		c.5461-10T>C (splice)	77	B
		c.4773+3A>G (splice)	84	B
Identical missense mutations				
c.5882G>A (p.Gly1961Glu)	51, 61	c.5882G>A (p.Gly1961Glu)	59, 52, 43, 57	B, C, D
c.1622T>C c.3113C>T (p.Leu541Pro p.Ala1038Val)	37, 44, 53, 59	c.1622T>C c.3113C>T (p.Leu541Pro p.Ala1038Val)	54, 56, 60, 65, 81	B
c.2588G>C (p.Gly863Ala)	44,59	c.2588G>C (p.Gly863Ala)	39	C

Supplementary Table 1: Summary of monoallelic severe and mild *ABCA4* mutations detected in this study and comparison with similar and equal mutations previously reported to be associated with the phenotype of late onset Stargardt disease (A)[4] or a subform of age-related macular degeneration (AMD) (B) with a specific pattern on fundus autofluorescence imaging (fine granular pattern with peripheral punctate spots; GPS),[5] and Stargardt disease with foveal sparing (C), early AMD (D),[6] late onset fundus flavimaculatus (E).[7] Studies were selected for comparison if an age of onset was specifically mentioned.

References:

1. Delori F, Greenberg JP, Fischer J, et al. Quantitative measurements of autofluorescence with the scanning laser ophthalmoscope. *Invest Ophthalmol Vis Sci* 2011;52:9379-9390.
2. Delori FC. Spectrophotometer for noninvasive measurements of intrinsic fluorescence and reflectance of the ocular fundus. *Applied Optics* 1994;33:7439-7452.
3. Greenberg JP, Duncker T, Woods RL, Smith RT, Sparrow JR, Delori FC. Quantitative fundus autofluorescence in healthy eyes. *Investigative ophthalmology & visual science* 2013;54:5684-5693.
4. Westeneng-van Haaften SC, Boon CJ, Cremers FP, Hoefsloot LH, den Hollander AI, Hoyng CB. Clinical and genetic characteristics of late-onset Stargardt's disease. *Ophthalmology* 2012;119:1199-1210.
5. Fritsche LG, Fleckenstein M, Fiebig BS, et al. A subgroup of age-related macular degeneration is associated with mono-allelic sequence variants in the ABCA4 gene. *Investigative ophthalmology & visual science* 2012;53:2112-2118.
6. Simonelli F, Testa F, de Crecchio G, et al. New ABCR mutations and clinical phenotype in Italian patients with Stargardt disease. *Investigative ophthalmology & visual science* 2000;41:892-897.
7. Souied EH, Ducroq D, Rozet JM, et al. A novel ABCR nonsense mutation responsible for late-onset fundus flavimaculatus. *Investigative ophthalmology & visual science* 1999;40:2740-2744.